GEOPHYSICAL RESEARCH LETTERS, VOL. 24, NO.11, PAGES 1291-1294, JUNE 1, 1997

Surface wave waveform inversions for local shear-wave velocities under eastern Australia

M. L. Passier

Department of Geophysics, Utrecht University, Utrecht, Netherlands

R. D. van der Hilst

Department of Earth, Atmospheric, and Planetary Sciences, MIT, Cambridge, USA

R. K. Snieder

Department of Geophysics, Utrecht University, Utrecht, Netherlands

Abstract. The waveform inversion method developed by *Kushnir et al.* [1989] and expanded by *Passier and Snieder* [1995b] yields estimates of structure along short interstation paths and of average velocity gradients. In contrast, 3D tomographic inversions yield local estimates of the earth structure by combining the information contained in a large set of long propagation paths. Both approaches lead to estimates of the local earth structure, but the two methods are subject to different types of artifact. As a test case of the consistency of the two approaches we consider the recent S-velocity model of the Australian region by *Zielhuis and Van der Hilst* [1996]. We invert 20 Rayleigh wave waveforms between 20 and 110 s recorded on the Australian continent, most of them by the mobile SKIPPY network. From the data, we directly extract measurements of the S-velocity structure at various short interstation paths in Australia and obtain estimates of the average velocity gradient along long paths. The estimates of the local interstation structure and the estimates of the velocity gradient are consistent with the 3D model of *Zielhuis and Van der Hilst* [1996]. These results provide illustrative examples of how specific features of a complex velocity structure can be determined using only a few waveforms.

Introduction

Broadband seismological data are an important tool for mapping the S-velocity in the mantle. Using the Partitioned Waveform Inversion developed by *Nolet* [1990], *Zielhuis and Van der Hilst* [1996] (hereafter referred to as ZH96) used data recorded by the SKIPPY array [*Van der Hilst et al.*, 1994; *Kennett and Van der Hilst*, 1996] to obtain a 3D model of the mantle under Australia. As an example, Figure 1 shows layers at depths of 140 and 300 km of a model which is based on the dataset collected in eastern Australia augmented by data from central north Australia.

Paper number 97GL01272.
0094-8534/97/97GL-01272$05.00

Every inversion method for retrieving earth structure suffers from artifacts. In the construction of models such as ZH96 numerous crossing paths eventually have led to the final model, while in the approach taken by *Passier*

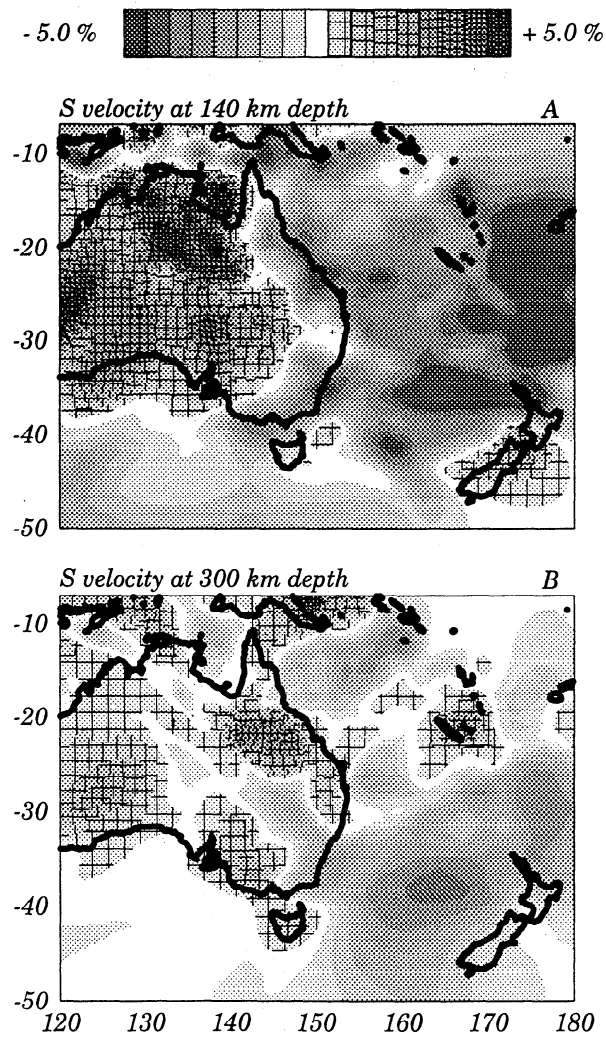

Figure 1. S velocity distributions at depths of (a) 140 km and (b) 300 km obtained after inversion of waveforms collected by the SKIPPY stations in eastern and central north Australia. Reference velocities are 4.5 and 4.66 km/s, respectively.

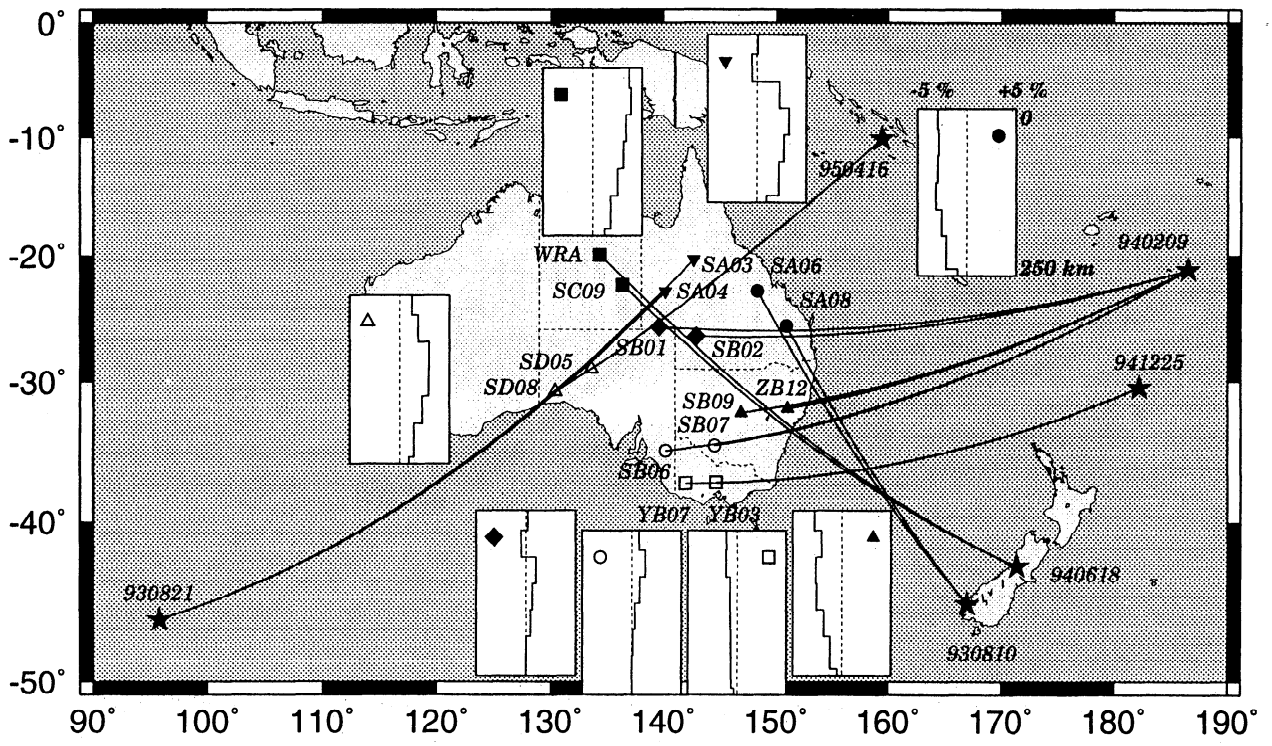

Figure 2. Stations, events, great circle paths, and inversion results for the case I inversions. In all velocity panels, perturbations range from −5% to 5% and depth ranges from 0 to 250 km.

and Snieder [1995b] (hereafter referred to as PS95b) a smaller number of data provides localized estimates the earth structure along short interstation paths. The artifacts produced by the two approaches will in general be different; the 3D tomographic approach may lead to blurring and underestimation of the local velocity perturbation, and errors in the source mechanism (*Muyzert and Snieder* [1996]) and source location can be mapped in velocity perturbations. In the approach taken by PS95b one measures the velocity along short paths so that the relative error in the obtained velocity perturbation could be larger. Effects of seismic anisotropy, which is not accounted for in either of these methods, will affect the velocity estimates in different ways in the two approaches. Similarly, both methods are subject to a (minor) velocity bias due to deviations of the propagation direction from the great-circle (e.g. *Alsina et al.* [1993], *Alsina and Snieder* [1996]), but this bias affects the velocity estimates obtained with the two approaches in a different way. The goal of this paper is not to quantify such uncertainties but to assess the robustness of some striking velocity estimates obtained from tomographic imaging, ZH96, by comparison with with structural information obtained with the waveform inversion method by PS95b.

Method and data

We used the surface wave waveform inversion method presented by PS95b to obtain relative S-velocity perturbations as a function of depth between pairs of stations. Station pairs (mostly of the SKIPPY array) were selected that are located on the same great circle as the source. Phase differences associated with the two fundamental mode Rayleigh wave waveforms were inverted for S-velocity perturbations on the path between the stations. The stations and events that were used for this so-called case I are shown in Figure 2. In this study, the stations within one pair are typically separated by 300 to 400 km. Alternatively, surface wave waveforms recorded in two stations at approximately the same epicentral distance, but with a slightly different azimuth to the source, were inverted for the relative path-averaged horizontal S-velocity gradient between the structures under the two paths. The stations and events used for this configuration, called case II, are shown in Figure 3. For case II, higher modes are incorporated in the waveform inversion to enhance the depth resolution with respect to the inversions of only fundamental mode data (PS95b). Information of all the events used is listed in Table 1. The reason why higher modes can be used in the Case II inversion but not in the Case I inversion is not quite clear to us. However, the numerical examples shown in the Figures 14BE of PS95b indicate that in the presence of higher modes the Case I inversion retrieves the fundamental mode excitation coefficients acccurately.

We used vertical component displacement waveforms in the period range between 20 and 110 s. To be able to compare two waveforms in the case II inversions, we corrected for differences in epicentral distance as described in PS95b. Throughout this study we used the same 1D reference model as was used for model ZH96. It has a crustal thickness of 30 km and is a slight modification of

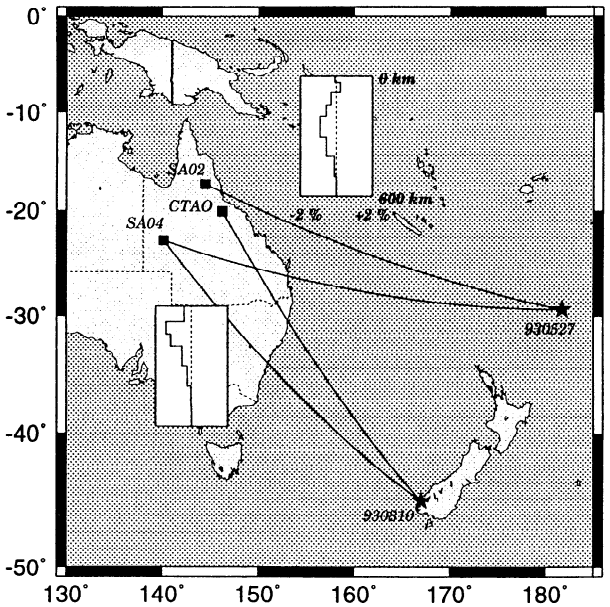

Figure 3. Stations, events, great circle paths, and inversion results (in both cases: northern path minus southern path) for the case II inversions. Note that the scale is different than that used in Figure 3: in all velocity panels, perturbations range from −2% to 2% and depth ranges from 0 to 600 km.

the PREM model of *Dziewonski and Anderson* [1981], see also *Zielhuis and Nolet* [1994].

In some inversions, regularization has been applied by adding the weighted depth integral of the squared velocity perturbations to the function to be minimized in the inversion. However, the weights given to the regularization term were small and do not significantly affect the estimates of the velocity perturbation (see PS95b, in particular Figures 3,5,7-9).

Results for Case I

Figure 2 shows the locations and results (velocity perturbations between two stations of each pair relative to the reference model) of the case I experiments. The vertical depth scale in each panel runs from the surface to 250 km and the velocity perturbations run from -5% to +5%. In PS95b, the vertical resolving power of the technique is discussed and it is shown that the crustal contamination below the Moho is small.

Our results along the easternmost edge of the continent (paths SA08 to SA06 and ZB12 to SB09) both reveal S velocities which are 2 to 3% lower than the reference model. These lower-than-average velocities persist from the surface down to a depth of at least 200 km. A dramatic change in the S-velocity structure in north Australia can be observed if we move from the eastern continental margin westward to the central part of the continent (paths SA04 to SA03 and SC09 to WRA). Both inversions yield S velocities which are 3 to 4% higher than the reference model down to a depth of at least 200 km. The structure between SA04 and SA03 seems to be only slightly perturbed down to 70 km depth. These results indicate a transition in north Australia from low upper mantle velocities in the east to high upper mantle velocities in the central part of the continent. Further to the south, we do not observe such a sharp transition if we move from the eastern margin in a westward direction. Instead, the inversion results (paths YB03 to YB07, SB07 to SB06, and SB02 to SB01) suggest a region with moderate S-velocity perturbations adjacent to the areas with pronounced low velocities in the east. Moving further westward in the southern part of the continent, we find high velocities again for the path between SD05 and SD08. The perturbations are strongest between 70 and 150 km depth where the amplitude is about 2 to 3%. These velocity anomalies correspond well with the features in the model of ZH96 obtained by PWI. At a depth of 80 km, our experiments as well as PWI reveal a lateral contrast of about 6% across the transition from the Phanerozoic eastern edge of the continent to the Proterozoic shield in the interior.

Results for Case II

Figure 3 shows the setting of the case II experiments and the path-averaged velocity contrasts relative to the reference model as obtained by inversion. The vertical depth scale in each panel runs from the surface to 600 km while the velocity perturbations run from -2% to +2%. Synthetic tests in PS95b demonstrate that for the employed frequencies the solution is reliable at least down to 400 km depth. Both inversions reveal higher velocities under the path to SA04 than under the paths to SA02 and CTAO, respectively (Figure 3). Inversion of the data of the 930527 event shows that the largest contrast between the paths to SA02 and SA04 is located between depths of 150 and 400 km. At shallower depth, the contrast is less pronounced. In contrast to this event, inversion of the data of the 930810 event reveals that the depth interval where the path to SA04 is faster than the path to CTAO is mainly restricted to shallower levels between 80 and 200 km (Figure 4).

The inversion method for case II provides an estimate of the weighted average of the velocity gradient perpendicular to the path. The fact that the oceanic structure can differ significantly from the reference model is not very important since the reference model is only used for the computation of the sensitivity kernels of the phase velocity with respect to the S-velocity perturbations. Possible large phase deviations generated by the difference between the true oceanic structure and the

Table 1. Events used

Date	Time	Lat	Lon	Depth	m_b/M_s	Region
93/05/27	08:52:00	29.4 S	178.0 W	128	5.9/–	Kermadec
93/08/10	00:51:55	45.0 S	166.7 E	15	6.2/7.1	S. Island (NZ)
93/08/21	08:07:50	46.3 S	95.8 E	15	5.0/–	SE. Indian Rise
94/02/09	19:27:09	21.2 S	173.5 W	21	5.6/5.2	Tonga
94/06/18	03:25:20	42.9 S	171.5 E	15	6.2/7.2	S. Island (NZ)
94/12/25	11:43:54	30.4 S	177.8 W	37	5.1/	Kermadec
95/04/16	13:23:48	10.1 S	159.4 E	23	5.6/5.7	Solomon Islands

reference model are absorbed in the excitation terms that are determined in the PS95b method. If we assume that the velocity contrast along the oceanic parts of the paths shown in Figure 3 is small (an assumption that is supported by Figure 1), then the results of the case II inversions lead to estimates of the velocity gradient along the continental part of the path only. Our inversion results, in combination with the orientation of the used paths, suggest a strong component of the velocity gradient from the northeast to the southwest in the uppermost mantle under northeast Australia. For the deeper levels, we find a strong component of the velocity gradient in the north-south direction. These observations correspond well with the structure obtained from PWI. Following the results of *Zielhuis and Van der Hilst* [1996], we conclude that it is most likely that the differences we observe in the waveforms are mainly caused by a dominating contrast, centered around 140 km depth, between low velocities along the northeastern continental margin and high velocities southwest of this low velocity belt.

We assumed that for both case II examples the measured gradients are from continental origin (i.e., no contributions from the parts where both paths travel through oceanic structure). This means that for both examples approximately one third of the total structure along each path must be the cause of the observed gradients. This implies that the analysis of the 930810 event suggests a contrast of about 3 to 4% in the uppermost mantle beneath the continent. This is less than the value suggested by the models obtained by PWI and by the case I experiments, which is about 6%. This discrepancy might be due to effects of structure along the oceanic parts of the paths. These effects have been assumed to be negligible, but might in reality contribute to a small part of the observed phase shifts. Analysis of the data of the 930527 event suggests a contrast of up to about 3% in the deeper areas of the region. This coincides well with the value according to the models obtained by PWI.

Conclusions

The waveform inversion method explained in PS95b has been used to obtain estimates of structure along short interstation paths and average velocity gradients in Australia. The results confirm the major characteristics of the model of the Australian region of ZH96 and provide illustrative examples of how specific features of a complex velocity model can be visualized and/or verified by applying the inversion technique of PS95b to only a few waveforms. For such a test, the role of the relatively short paths between the stations in the case I examples is crucial. The use of short paths increases the resolution by reducing the low-pass character of the data [*Passier and Snieder,* 1995a]. Since structural differences directly translate into observable phase differences between recorded waveforms, the examples in this paper not only demonstrate the possibility of using the method as an independent testing tool, but the technique also provides a way to obtain results that can be used as constraints in subsequent large-scale inversions of much larger datasets.

Acknowledgments. The critical and constructive comments of three reviewers are very much appreciated. This work was done at MIT, Cambridge MA, USA. We thank them for providing the facilities. We also thank NATO for supporting this project financially through grant CRG 951225. This is Geodynamics Research Institute (Utrecht University) contribution 97.005.

References

Alsina, D., and R. Snieder, 1996, Constraints on the velocity structure beneath the Tornquist-Teisseyre zone from beamforming analysis, *Geophys. J. Int.,* **126**, 205-218.

Alsina, D., R. Snieder, and V. Maupin, 1993, A test of the great circle approximation in the analysis of surface waves, *Geophys. Res. Lett.,* **20**, 915-918.

Dziewonski, A.M. and D.L. Anderson, 1981, Preliminary reference earth model, *Phys. Earth Planet. Int.,* **25**, 297-356.

Kennett, B.L.N. & Van der Hilst, R.D., 1996. Using a synthetic continental array in Australia to study the Earth's interior, *J. Phys. Earth,* in press.

Kushnir, A.F., A.L. Levshin and D.E. Lokshtanov, 1989, Determination of a regional velocity structure from surface wave seismograms recorded at a set of stations, in *Proceedings of the Sixth International Mathematical Geophysics Seminar*, vol. 3, pp. 489-498, Free Univ., Berlin, Germany.

Muyzert, E.J., and R.K. Snieder, 1996, The influence of errors in the source parameters on phase velocity measurements of surface waves, *Bull. Seismol. Soc. Am.,* **86**, 1863-1872.

Nolet, G., 1990. Partitioned waveform inversion and two-dimensional structure under the Network of Autonomously Recording seismographs, *J. geophys. Res.,* **95**, 8499–8512.

Passier, M.L. & Snieder, R.K., 1995a. On the presence of intermediate-scale heterogeneity in the upper mantle, *Geophys. J. Int.,* **123**, 817–837.

Passier, M.L. & Snieder, R.K., 1995b. Using differential waveform data to retrieve local S velocity structure or path-averaged S velocity gradients, *J. geophys. Res.,* **100**, 24061–24078.

Shaw, R.D., Welmann, P., Gunn, P., Whitaker, A.J., Tarlowski, C. & Morse, M.P., 1995. Australian Crustal Elements Map, *AGSO Research Newsletter,* **23**, 1–3.

Van der Hilst, R.D., Kennett, B.L.N., Christie, D. & Grant, J., 1994. SKIPPY: Mobile broad-band arrays to study the seismic structure of the lithosphere and mantle beneath Australia, *EOS Trans. Am. Geophys. Un.,* **75**, 177 & 180–181.

Zielhuis, A. & Nolet, G., 1994. Shear-wave velocity variations in the upper mantle beneath Central Europe, *Geophys. J. Int.,* **117**, 695–715.

Zielhuis, A. & Van der Hilst, R.D., 1996. Upper mantle shear velocity beneath eastern Australia from inversion of waveforms from SKIPPY portable arrays, *Geophys. J. Int.,* **127**, 1–16.

M.L. Passier and R.K. Snieder, Department of Geophysics, Utrecht University, PO Box 80.021, 3508 TA, Utrecht, Netherlands. (e-mail: snieder@geof.ruu.nl)

R.D. van der Hilst, Department of Earth, Atmospheric, and Planetary Sciences, Massachusetts Institute of Technology, Rm. 54–514, Cambridge MA 02139, USA.

(received August 23, 1996; revised March 17, 1997; accepted April 9, 1997.)